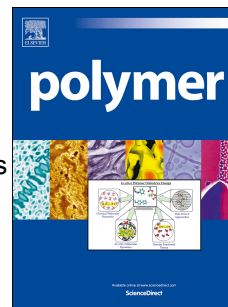


Accepted Manuscript

Aggregation-induced CPL response from chiral binaphthyl-based AIE-active polymers
via supramolecular self-assembled helical nanowires

Jing Ma, Yuxiang Wang, Xiaojing Li, Lan Yang, Yiwu Quan, Yixiang Cheng



PII: S0032-3861(18)30292-1

DOI: [10.1016/j.polymer.2018.04.006](https://doi.org/10.1016/j.polymer.2018.04.006)

Reference: JPOL 20486

To appear in: *Polymer*

Received Date: 20 January 2018

Revised Date: 28 March 2018

Accepted Date: 2 April 2018

Please cite this article as: Ma J, Wang Y, Li X, Yang L, Quan Y, Cheng Y, Aggregation-induced CPL response from chiral binaphthyl-based AIE-active polymers *via* supramolecular self-assembled helical nanowires, *Polymer* (2018), doi: 10.1016/j.polymer.2018.04.006.

This is a PDF file of an unedited manuscript that has been accepted for publication. As a service to our customers we are providing this early version of the manuscript. The manuscript will undergo copyediting, typesetting, and review of the resulting proof before it is published in its final form. Please note that during the production process errors may be discovered which could affect the content, and all legal disclaimers that apply to the journal pertain.

Graphical Abstract

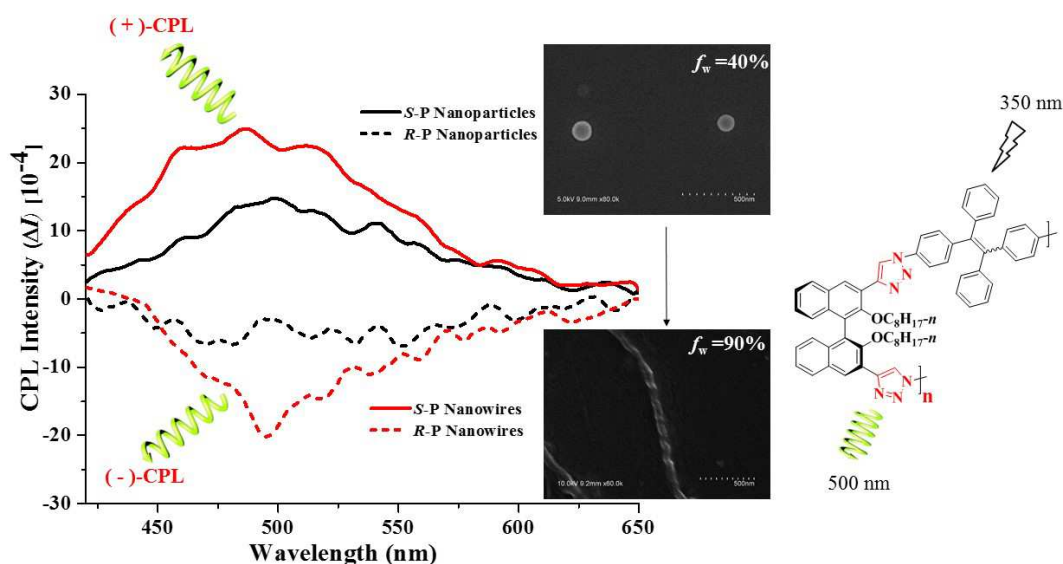
Aggregation-induced CPL Response from Chiral Binaphthyl-based AIE-active Polymers *via* Supramolecular Self-assembled Helical Nanowires

Jing Ma,[†] Yuxiang Wang,[†] Xiaojing Li,[†] Lan Yang,[†] Yiwu Quan,^{†,*} and Yixiang Cheng^{†,*}

[†] Key Lab of Mesoscopic Chemistry of MOE, Collaborative Innovation Center of Chemistry for Life Sciences, School of Chemistry and Chemical Engineering, Nanjing University, Nanjing 210023, China

E-mail: yxcheng@nju.edu.cn; quanyiwu@nju.edu.cn

Chiral conjugated polymer enantiomers incorporating 1,1'-binaphthyl and tetraphenylethene (TPE) can exhibit strong CPL signals due to the formation of the supramolecular self-assembled helical nanowires in the aggregate.



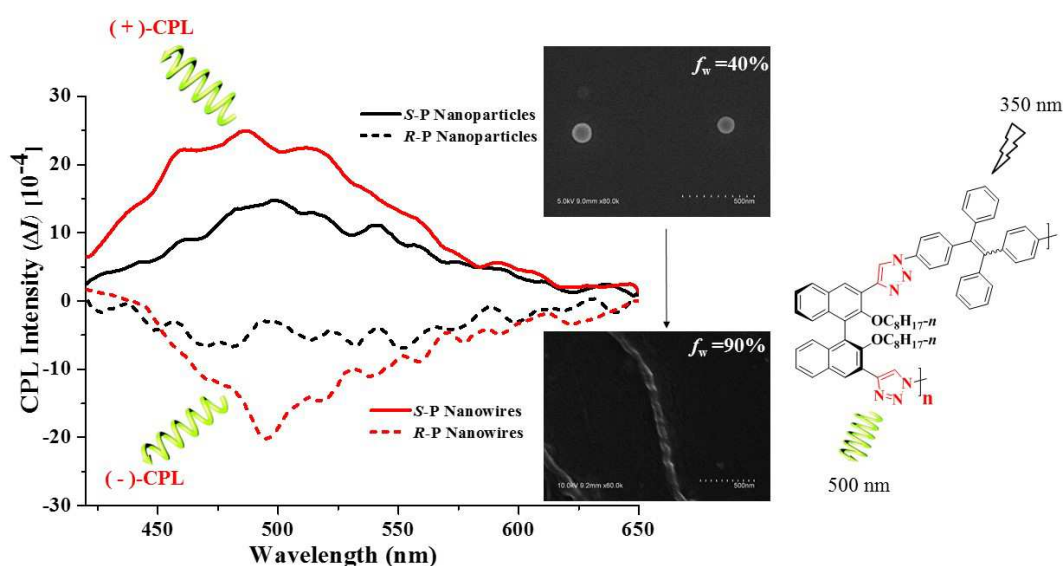
Aggregation-induced CPL Response from Chiral Binaphthyl-based AIE-active Polymers *via* Supramolecular Self-assembled Helical Nanowires

Jing Ma,[†] Yuxiang Wang,[†] Xiaojing Li,[†] Lan Yang,[†] Yiwu Quan,^{†,*} and Yixiang Cheng^{†,*}

[†] Key Lab of Mesoscopic Chemistry of MOE, Collaborative Innovation Center of Chemistry for Life Sciences, School of Chemistry and Chemical Engineering, Nanjing University, Nanjing 210023, China

E-mail: yxcheng@nju.edu.cn; quanyiwu@nju.edu.cn

Graphical Abstract



In this paper chiral polymer **R-P** could be synthesized by click polymerization reaction of (*R*)-3,3'-diethynyl-2,2'-bis(octyloxy)-1,1'-binaphthalene (**R-M-1**) and 1,2-bis(4-azidophenyl)-1,2-diphenylethene (**M-2**), and **S-P** was obtained by click polymerization reaction of (*S*)-3,3'-diethynyl-2,2'-bis(octyloxy)-1,1'-binaphthalene (**S-M-1**) and **M-2**, respectively. **R-/S-P** enantiomers can show strong aggregation-induced circularly polarized luminescence (AICPL) emission signals in the aggregate and cast-spin film, and the dissymmetry factors (g_{lum}) can be up to 6.97×10^{-3} and 1.45×10^{-2} , respectively. The SEM images further

demonstrate that AICPL response behavior of **R/S-P** can be attributed to the formation of the supramolecular self-assembled helical nanowires in the aggregation state at 90% of the fraction of water (f_w).

Introduction:

In the past decades, more and more efforts have been devoted to the chiral conjugated polymers since the polymer chain backbone with the delocalizable π -electronic structures and molecular wire features can greatly amplify the fluorescence response signals through facile energy migration along the polymer backbone upon the light excitations.^[1] Currently, chiral conjugated polymers have attracted increasing attentions on their optical functions,^[2] especially circularly polarized luminescence (CPL) materials, which can be regarded as the selective emission of left- and right-handed polarized light. Normally, chiral feature signals (CD, CPL, and so on) can be effectively amplified *via* the synergic effect between the conjugated polymer backbone structure and chiral moiety.^[3] Considering the potentially significant application of CPL materials, such as biomedical diagnosis,^[4] cell imaging^[5] and catalysts for asymmetric photochemical synthesis,^[6] developing novel chiral conjugated polymers is of great importance.

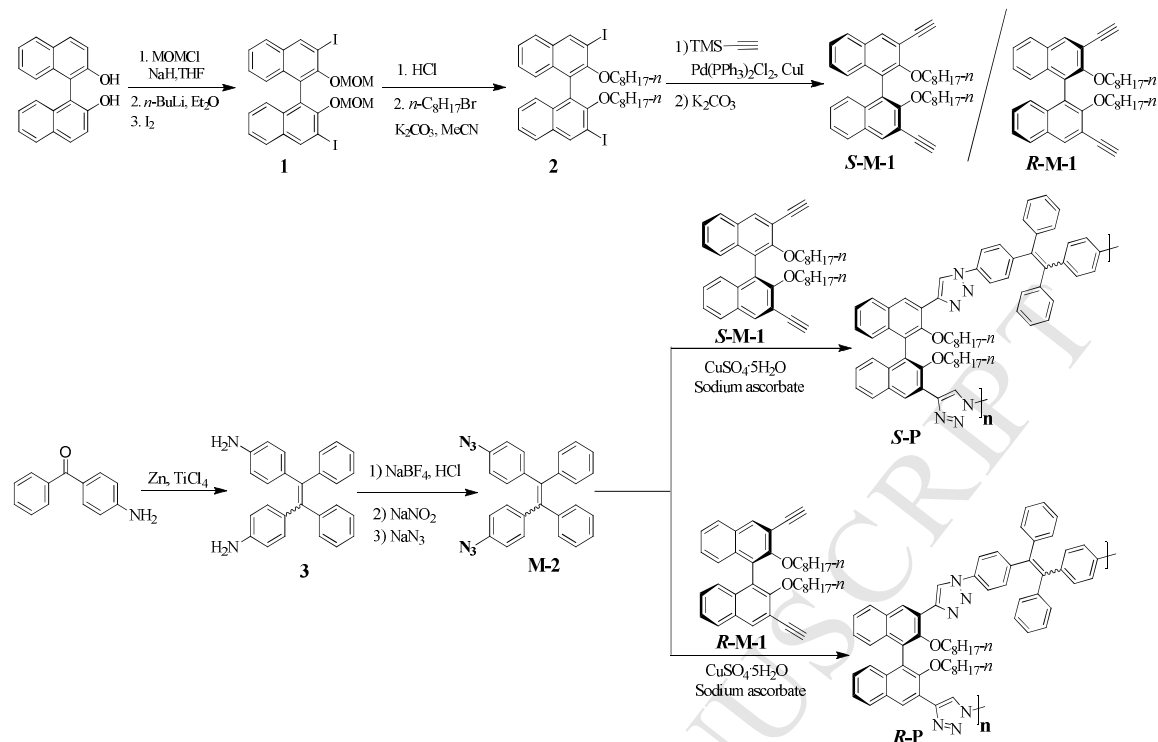
In 2001 aggregation-induced emission (AIE) was firstly proposed by Tang, illustrating the phenomenon that almost no luminescence can be observed in solution, but stronger emission happened in aggregate or solid state.^[7] Recently, there have been more and more reports on AIE-active functional materials for chemosensors, biological imaging,^[8] fluorescent probe^[9] and OLED devices.^[10] Tang's group first reported a small molecule containing an AIE-active silole core and chiral sugar pendants, which exhibited great g_{lum} value up to -0.12 and -0.08 in

heterogeneous suspension and neat static cast film.^[11] Recently, Liu's group also found a general approach for fabricating 1D aggregation-induced CPL (AICPL) nanoassemblies of 1,3,5-benzenetricarbonyl-based L-glutamate diethyl ester and styrylbenzene derivatives, which successfully encapsulated guest achiral AIE dyes into the chiral space.^[12] Although Tang's group reported some AICPL materials based on chiral AIE-active small molecules, so far there have been very few works on AIE-active chiral conjugated polymers as AICPL materials.^[13] Chiral 1,1'-binaphthol (**BINOL**) have been widely used as the starting materials for the synthesis of chiral conjugated polymers with main chain chiral configuration. These binaphthyl-based polymers can exhibit efficient and stable chiral configuration as well as high chiral induction, which represents a new generation of materials for asymmetric catalysis^[14] and enantioselective recognition.^[15] Besides, click reactions, represented by the copper(I)-catalyzed azide-alkyne cycloaddition (CuAAC), have been successfully employed to design various functional materials due to their feasibility, selectivity, and high-yield,^[16] especially involving in the fabrication of biological materials^[17] and chiral materials.^[18] Our group first synthesized chiral conjugated polybinaphthyls *via* click polymerization reaction, this kind of polymers containing a triazole moiety in the polymer main chain backbone could show high sensitivity and selectivity for Hg²⁺ recognition.^[19] Recently our group developed tunable green AICPL materials of three-component chiral binaphthyl-based conjugated polymers *via* FRET mechanism from fluorene moiety to AIE-active TPE chromophore.^[13a] To our best knowledge, so far there has been no report on AICPL material based on AIE-active chiral conjugated polymers *via* click polymerization reaction. Herein, we designed and synthesized the novel AIE-active chiral binaphthyl-based polymer enantiomers **R/S-P** by using click polymerization reaction, and strong AICPL response behavior

can be attributed to the formation of the supramolecular self-assembled helical nanowires in the aggregation state. We believe that these AIE-active chiral conjugated polymers will be regarded as one of the most promising candidate materials for CPL emitters on optical sensor, 3D display and other photoelectric functional applications.

Results and discussions

The detailed synthesis procedures of polymers **R/S-P** are outlined in Scheme 1. Two chiral monomers, (*R*- or *S*-)-3,3'-diethynyl-2,2'-bis(octyloxy)-1,1'-binaphthalene (**R-M-1** or **S-M-1**) and AIE-active monomer, 1,2-bis(4-azidophenyl)-1,2-diphenylethene (**M-2**), could be synthesized according to the reported literatures.^[20] Chiral polymer **R-P** could be synthesized by click polymerization reaction (specifically Azide-Alkyne Huisgen Cycloaddition) of **R-M-1** and **M-2** in about 76% yield, and chiral polymer **S-P** was obtained by click polymerization reaction of **S-M-1** and **M-2** in about 80% yield. The thermal stability of **R-P** is evaluated by thermogravimetric analysis (TGA). It loses 5% of its original weight when it is heated to a temperature of about 330 °C (T_d), which indicates better thermal stability. In addition, the resulting polymers have moderate yields and molecular weights (**R-P**: M_n = 9240, PDI = 1.43; **S-P**: M_n = 8227, PDI = 1.41). In the ¹H NMR spectrum of **R/S-P**, the peaks at 3.31 ppm from the acetylene proton resonance completely disappear, which can also demonstrate the effective click polymerization reaction between chiral monomer **M-1** and **M-2**. The target product can also show excellent solubility in common solvents, such as THF, CH₂Cl₂, CHCl₃, which can be due to the flexible *n*-octyl group substituents from binaphthyl moiety.



Scheme 1. Synthesis procedures of *S-M-1*, *R-M-1*, *M-2*, *R-P* and *S-P*.

In this paper, we first investigated their UV-*vis* absorption and fluorescent emission spectra in THF and THF-H₂O mixed solvents at a fixed concentration (5.0×10^{-5} mol L⁻¹ corresponding to binaphthyl moiety), respectively. As shown in Figure 1, *R/S-P* have two absorption bands at 255 nm and 298 nm, which can be regarded as the π - π^* transition of binaphthyl moiety. The maximum UV-*vis* absorption λ_{\max} wide band centered at around 345 nm can be assigned to the conjugated polymer backbones. Furthermore, UV-*vis* absorption spectra were carried out by changing the different water fraction (f_w) in THF-H₂O mixtures. As f_w increases to 80%, obvious red shift (about 8 nm) can be observed relative to the absorption band in pure THF solution. The relative intensity of absorption peaks doesn't show obvious change until poor solvent water fraction f_w increases up to 90%. But as the further increase of water, the whole UV-*vis* absorption shows great decrease at $f_w = 95\%$ and 99% , which may be attributed to the reason that the polymer aggregate nanoparticles tend to form the precipitation at high water fraction.

As is evident from Figure 2, we found that **R-/S-P** in THF solution show weak fluorescence emission centered at 435 nm with 1.3% of quantum yield. Upon the addition of water, AIE-active **R-/S-P** can emit the gradual enhancement fluorescence signal with 60 nm red-shift to 495 nm and reach the strongest emission intensity ($\Phi_{\text{PL}}=12.3\%$) at $f_w = 80\%$, which can be assigned to the effective π - π^* conjugated effect in the aggregate state. As shown in the insert of Figure 2, bright blue-green color can be clearly observed under a commercially available UV lamp. But like UV-*vis* absorption, the fluorescence signals appear obvious decrease as the further increase of water at $f_w = 90\%$, 95% and 99%.

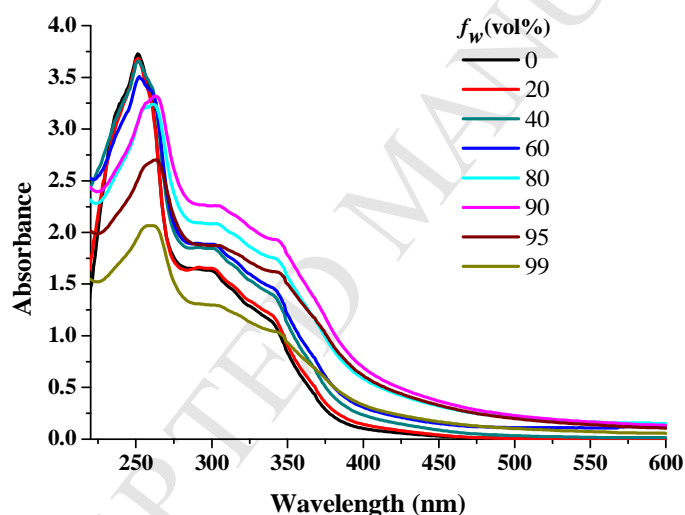


Figure 1. UV-*vis* absorption spectra of **R-/S-P** in THF-water mixtures at a fixed concentration ($5.0 \times 10^{-5} \text{ mol L}^{-1}$, scanning rate: 200 nm/min, cell length: 10 mm).

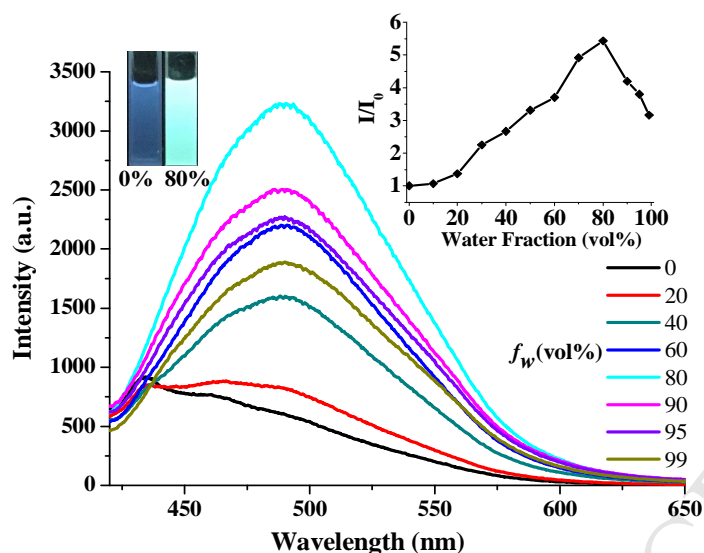


Figure 2. Fluorescence emission spectra of *R-/S-P* in THF-water mixtures at a fixed concentration ($5.0 \times 10^{-5} \text{ mol L}^{-1}$, $\lambda_{\text{ex}} = 350 \text{ nm}$, bandwidth for emission: 5 nm, bandwidth for excitation: 5 nm, scanning rate: 200 nm/min, cell length: 10 mm). Inset: Plot of (I/I_0) values *versus* the compositions of the aqueous mixtures.

The CD spectra of *R-/S-P* were performed in THF solution ($5.0 \times 10^{-5} \text{ mol L}^{-1}$) and exhibits clear mirror image CD bands (Figure 3). According to the reported literature, the chiral BINOL can exhibit three characteristic CD signals, one weaker band at around 300 nm and two stronger bands at about 225 nm and 240 nm.^[21] Taken *S-P* as an example, the CD spectra display three obvious peaks at 250 nm, 267 nm and 342 nm. Among them, strong negative Cotton effects at 250 nm and positive Cotton effects at 267nm can be assigned to the feature skeleton absorption of (*S*)-binaphthyl moiety in the main chain of the polymer, while the long wavelength CD effect appears at 342 nm, which can be regarded as the extended conjugated structure in the repeating unit and a high rigidity of polymer backbone. The absorption dissymmetry factor (g_{abs}), which defined as $g_{\text{abs}} = 2(\epsilon_{\text{L}} - \epsilon_{\text{R}}) / (\epsilon_{\text{L}} + \epsilon_{\text{R}}) = \Delta\epsilon/\epsilon$, can reach as high as 5.78×10^{-4} for *S-P* and -6.25×10^{-4} for *R-P*, respectively. To further investigate the CD spectrum change feature of *R-/S-P* in the aggregate state, we found that the intensity of CD signal gradually declines as the increase of water fraction over 40%, which may be due to the concentration decrease of the dispersed polymer

chains in THF-H₂O mixed system.

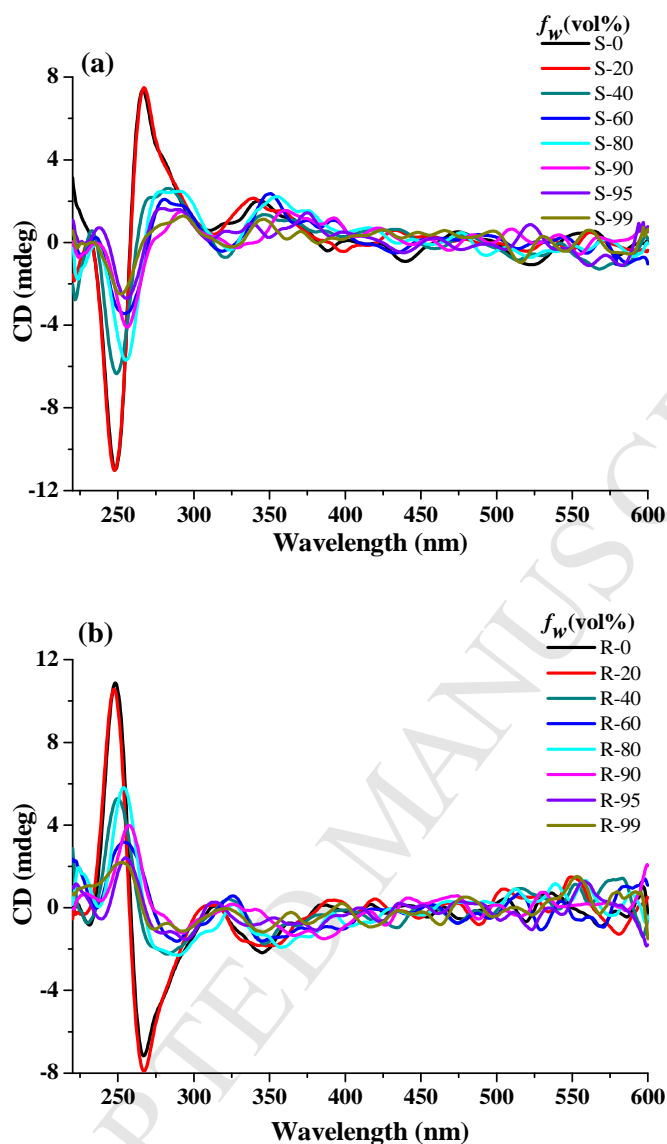


Figure 3. CD spectra of (a) **R-P** and (b) **S-P** in THF and THF-water mixtures at a fixed concentration ($5.0 \times 10^{-5} \text{ mol L}^{-1}$, scanning rate: 200 nm/min, cell length: 1 mm)

The AIE-active conjugated polymers **R/S-P** can display strong aggregation-induced fluorescence enhancement responses in the aggregate state, which inspires us to further investigate their aggregation-induced CPL behaviour. Seen as a fundamental parameter of CPL, the luminescence dissymmetry factor (g_{lum}) value can be evaluated by using the equation $g_{\text{lum}} = 2(I_L - I_R)/(I_L + I_R)$, where I_L and I_R are the emission intensities of left and right circularly polarized luminescence, respectively. As is evident from Figure 4, almost no CPL emission signal can be detected in THF

solution because **R/S-P** are nearly non-luminescent. However, **R/S-P** appear obvious CPL response signal ($g_{\text{lum}} = -1.87 \times 10^{-3}$ for **R-P**, $+4.12 \times 10^{-3}$ for **S-P**) at $f_w = 40\%$, indicating the gradual intramolecular chirality transfer *via* the conjugated polymer chain backbone structure. Meanwhile, it can be found that the aggregation-induced CPL of polymers **R/S-P** can exhibit good mirror-image, and the emission peak situated at 490 nm-500 nm can also coincide well with their fluorescence spectra in the aggregate state. The AICPL signals can reach the strongest emission ($g_{\text{lum}} = -5.64 \times 10^{-3}$ for **R-P**, $+6.97 \times 10^{-3}$ for **S-P**) at $f_w = 90\%$, but tend to decrease (Figure S10) while the further addition of water to 99% ($g_{\text{lum}} = -4.12 \times 10^{-3}$ for **R-P**, $+4.26 \times 10^{-3}$ for **S-P**) due to the precipitate formation at high H₂O fraction. We infer that the AIE-active **R/S-P** can form the regular and orderly self-assembly nanoparticles in the aggregate state leading to AICPL emission enlargement effect. ^[11]

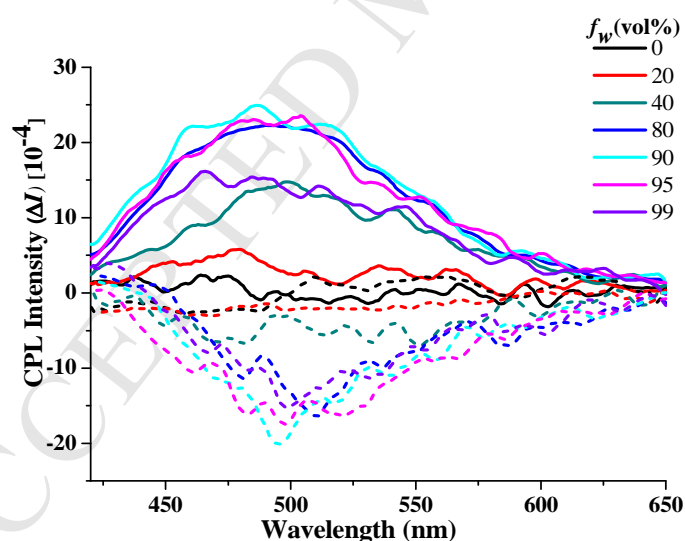


Figure 4. CPL spectra of **R/S-P** in THF and THF-water mixtures at a fixed concentration ($5.0 \times 10^{-5} \text{ mol L}^{-1}$, $\lambda_{\text{ex}} = 350 \text{ nm}$, bandwidth for emission: 3000 nm , bandwidth for excitation: 3000 nm , scanning rate: 200 nm/min , cell length: 10 mm).

To well understand the AICPL response enhancement mechanism of the polymers **R/S-P** in the aggregation, we further investigated the morphologies of aggregates in different THF-H₂O mixtures by using scanning electron microscopy (SEM) measurements. In the supramolecular

self-assemble process, we found that the surface profile of free polymer chain forms regularly sphere nanoparticles at $f_w = 40\%$ (Figure 5a). As the further increase of water fraction up to $f_w = 80\%$, the sphere aggregates of **S-P** gradually transform as left-handed helical nanowires *via* supramolecular self-assembly as shown in Figure 5b. Interestingly, these supramolecular self-assembled helical nanowires appear more twisted nanowires (Figure 5c) at $f_w = 90\%$ and even intertwine with each other (Figure 5d) at $f_w = 95\%$. As is evident from Figure S15, the helical nanofibers further coiled in the end to form several irregular rings as the increase of water fraction up to 99%. We can draw the conclusion that obvious decrease of UV-*vis* absorption, CD, fluorescence and AICPL emission signals can be attributed to the precipitate formation at high poor solvent fraction. As shown in Figure S12, we also observed that **R-P** self-assembled the same left-handed helical nanowires as **S-P** in the THF-H₂O mixtures. No expected handedness inversion indicates that the driving force for the formation of helical nanowires are not only from the π - π interactions influenced by binaphthyl chirality, but also from the cooperate effects of multiple intermolecular hydrogen bonding (N-H \cdots O, C-H \cdots O, C-H \cdots N) and steric effects.^[22]

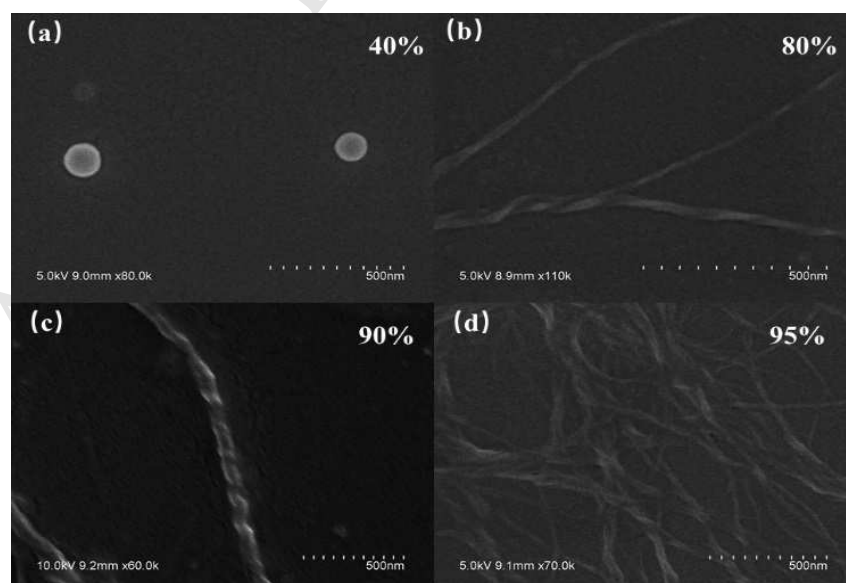


Figure 5. SEM images of **S-P** at (a) 40, (b) 80, (c) 90, (d) 95 vol% (f_w)

Considering that practical applications in emitting devices usually demand a solid state active

layer, we explored CPL emission of polymers **R/S-P** in the cast-spin film. As shown in Figure 6, **R/S-P** in the cast-film can exhibit stronger CPL response than in the solution at around 490 nm. Compared with the maximum response in solution, the g_{lum} values of **S-P** and **R-P** in the cast-spin film are 1.45×10^{-2} and 0.82×10^{-2} , amplified up to 2.08 times and 1.45 times respectively. Taking note of the fact that stronger π - π interactions between polymers will be created in the solid state in contrast to in the solution system, we suppose that the amplification effect in the cast-spin film is caused by the more highly ordered aggregated structures.^[11,23,24]

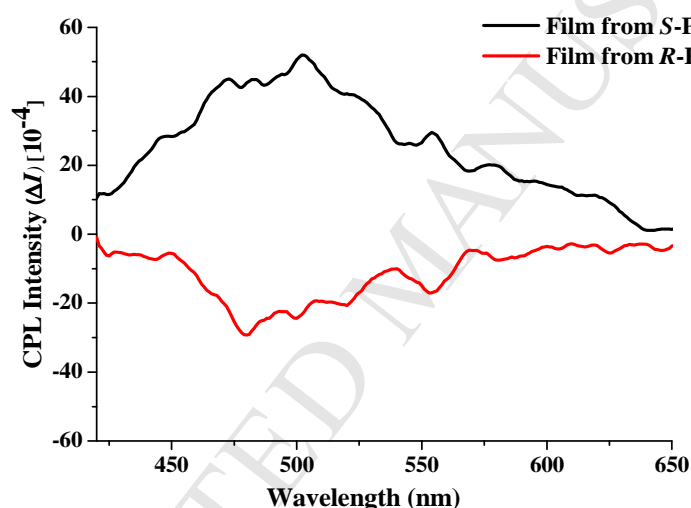


Figure 6. CPL spectra of **R/S-P** in the cast-spin film ($\lambda_{ex} = 350$ nm, bandwidth for emission: 3000 μ m, bandwidth for excitation: 3000 μ m, scanning rate: 200 nm/min).

Conclusions

In summary, we have designed and synthesized a pair of AIE-active chiral conjugated polymers enantiomers *via* click reaction. The CD and CPL spectra reveal the effective chiral transfer from chiral binaphthal moieties to AIE-active TPE chromophore *via* conjugated chain backbone structure. The dissymmetry factor g_{lum} can reach as high as 6.97×10^{-3} and 1.45×10^{-2} in the aggregate and cast-spin film, respectively. The SEM images show that chiral conjugated polymers

R/S-P can self-assemble as helical nanowires leading to the AICPL response behavior at particular THF-H₂O mixtures.

Experimental Section

Measurements and materials.

All the solvents and reagents were commercially available and analytical grade. THF and Et₃N were distilled from sodium in the presence of benzophenone. NMR spectra were obtained by using Bruker AVANCE III-400 spectrometer with 400 MHz for ¹H NMR and 100 MHz for ¹³C NMR, and the chemical shifts are reported as parts per million (ppm) relative to tetramethylsilane (TMS) as internal standard. Circular dichroism (CD) spectra were recorded on a JASCO J-810 spectropolarimeter, and the length of the sample cell was 0.1 cm. Circularly polarized luminescence (CPL) spectra were recorded with a JASCO CPL-300 spectrofluoropolarimeter. In the CPL measurements, the excitation wavelength was 350 nm, scan speed was 200 nm/min, number of scans was 1, and slit width was 3000 μm. The magnitude of circular polarization in the excited state is defined as $g_{lum} = 2(I_L - I_R)/(I_L + I_R)$, where I_L and I_R indicate the output signals for left and right circularly polarized light, respectively. Experimentally, the value of g_{lum} is defined as $g_{lum} = \Delta I/I = [\text{ellipticity}/(32980/\ln 10)]/(\text{unpolarized PL intensity})$ at the CPL extremum. Molecular weight was determined by gel permeation chromatography (GPC) with a Waters 244 HPLC pump, and THF was used as solvent relative to polystyrene standards. Dynamic light scattering (DLS) measurement was performed on a 90Plus particle size analyzer (Brookhaven Instruments Co.). Thermogravimetric analyses (TGA) were obtained from a Perkin-Elmer Pyris-1 instrument under N₂ atmosphere.

Synthesis of 3,3'-diethynyl-2,2'-bis(octyloxy)-1,1'-binaphthalene (M-1):

Monomer **M-1** was synthesized according to the reported literature. A mixture of compound **2** (2.00 g, 2.62 mmol), ethynyltrimethylsilane (1.28 g, 13.08 mmol), Pd(PPh₃)₂Cl₂ (183.61 mg, 10% mmol), CuI (49.82 mg, 10% mmol) were added to 10 mL Et₃N under N₂ atmosphere. The reaction was stirred at 80 °C for 24 h. After cooling to room temperature, the reaction mixture was filtered through a short silica gel column. The solvent was removed to afford crude intermediate product. K₂CO₃ (3.91 g, 28.29 mmol) were added into the mixed solvents of 10 ml CH₂Cl₂ and 10 ml CH₃OH and the previous intermediate product was added. The reaction was stirred overnight and extracted with CH₂Cl₂, washed with brine and dried over anhydrous Na₂SO₄. Then the solvent was removed, the crude product was purified by column chromatography (petroleum ether) to afford 0.85 g as a white solid in 58% yield. ¹H NMR (400 MHz, CDCl₃): δ 8.16 (s, 2H), 7.83 (d, *J* = 8.2 Hz, 2H), 7.39 (m, *J* = 8.2, 7.1, 1.2 Hz, 2H), 7.26 (m, *J* = 7.1, 1.2 Hz, 2H), 7.14 (d, *J* = 8.2 Hz, 2H), 4.00 (m, *J* = 8.7, 6.3 Hz, 2H), 3.70 (m, *J* = 8.7, 6.3 Hz, 2H), 3.31 (s, 2H), 1.36 – 1.15 (m, 8H), 1.15 – 1.04 (m, 4H), 1.04 – 0.95 (m, 4H), 0.95 – 0.74 (m, 12H), 0.71 – 0.56 (m, 2H). ¹³C NMR (100 MHz, CDCl₃): δ 155.61, 135.11, 134.31, 130.06, 127.84, 127.41, 126.02, 125.43, 125.30, 116.73, 81.27, 80.98, 77.48, 77.16, 76.84, 73.84, 31.85, 30.08, 29.27, 29.18, 25.55, 22.83, 14.29.

Synthesis of 1,2-bis(4-azidophenyl)-1,2-diphenylethene (M-2):

In a 100 mL three necked round bottom flask were placed 5.7 mL of distilled water and sodium tetrafluoroborate (1.35 g, 12.5 mmol). The mixture was stirred until all solid was dissolved, and then 5.7 mL of conc hydrochloric acid was added. The flask was placed in a -20 °C cold bath and the solution was kept stirring. In a separate flask containing 9.4 mL of distilled water were placed compound **3** (1.67 g, 4.61 mmol) and sodium nitrite (0.69 g, 10.02 mmol) (minimal heating was used to dissolve solids). The solution of compound **3** was added dropwise to the reaction flask

with stirring. The temperature was kept at -20 °C to -15 °C during the addition. The mixture was stirred for an additional 30 min. The precipitate was collected by filtration, washed with water followed by ethyl ether, and air dried to give brown solid which was used in next step. In a 200 ml round bottom flask were placed 38.5 ml of distilled water and sodium azide (0.47 g, 7.23 mmol). The flask was kept in an ice bath and the previous brown solid was added. The solution was kept stirring for 30 min and precipitations appeared on the bottom of the flask, which were collected through filtering to afford crude product (**M-2**) for further purification. The crude product can be dissolved in ether and filtered. After the filtrate was evaporated, the residue was purified by column chromatography to give 1.03 g as a yellow solid in 54% yield. ¹H NMR (400 MHz, CDCl₃): δ 7.18-7.11 (m, 6H), 7.05-6.94 (m, 8H), 6.81-6.70 (m, 4H). ¹³C NMR (100 MHz, CDCl₃): δ 143.44, 140.55, 140.33, 138.19, 132.86, 131.42, 128.09, 126.93, 118.50.

Synthesis of polymer R-/S-P:

M-1 (114.82 mg, 0.21 mmol), **M-2** (85.17 mg, 0.21 mmol), Na Ascorbate (16.28 mg, 40 mol%), CuSO₄·5H₂O (10.26 mg, 20 mol%) were added into the mixed solvents of 6 ml THF and 6 ml H₂O. The solution was stirred at 45 °C for 4 days under N₂. The solvents were removed under reduced pressure and the residue was extracted with CHCl₃ (2 × 50 mL). The organic layer was washed with an aqueous NH₄OH solution, water and then dried over anhydrous Na₂SO₄. After the solution was removed, the resulting polymer was precipitated into methanol, and then filtered and washed with methanol several times. The dark yellow polymers were collected and dried in vacuum to give **R-P** of 152.0 mg in 76% yield and **S-P** of 160.3 mg in 80% yield. $[\alpha]_D^{25}$ of **R-P** and **S-P** (THF, 1.0 g/1000 ml) are -282.0 and +328.0, respectively; GPC of **R-P**: M_w = 13200, M_n = 9240, PDI = 1.43, GPC of **S-P**: M_w = 11600, M_n = 8227, PDI = 1.41; Degradation temperature of **R-/S-P**:

$T_d = 330\text{ }^\circ\text{C}$; $^1\text{H NMR}$ (400 MHz, CDCl_3): δ 8.87 (d, $J = 19.2$ Hz, 2H), 8.51 (d, $J = 15.2$ Hz, 2H), 7.95 (d, $J = 7.8$ Hz, 2H), 7.51 (t, $J = 13.7$ Hz, 2H), 7.35 (d, $J = 6.9$ Hz, 2H), 7.25 – 6.90 (m, 18H), 3.52 (s, 2H), 3.15 (s, 2H), 1.24 – 0.91 (m, 10H), 0.82 (m, $J = 18.8, 6.9$ Hz, 4H), 0.77 – 0.50 (m, 16H), 0.38 (s, 2H).

Spin coating of thin polymer films:

Two films of *S-P* and *R-P* samples on ITO-coated glass substrate could be prepared by using spin-coating method. The corresponding chiral polymer layer is spin-coated from a 10 mg/ml solution in DMF on ITO-coated glass substrate. The spin speed was gradually increased to 1500 r/min and the spin lasted for about one minute.

Acknowledgment.

This work was supported by the National Natural Science Foundation of China (21674046, 21474048 and 51673093).

Supporting Information.; UV-*vis* absorption, fluorescence, CD and CPL spectra mentioned in above paragraphs; TGA, GPC and DLS data, SEM images and $^1\text{H NMR}$ spectra of new polymers as well.

Reference

- [1] (a) D. T. McQuade, A. E. Pullen, T. M. Swager, *Chem. Rev.* 100 (2000) 2537-2574; (b) S. W. Thomas III, G. D. Joly, T. M. Swager, *Chem. Rev.* 107 (2007) 1339-1386.
- [2] (a) S. T. Duong, M. Fujiki, *Polym. Chem.* 8 (2017) 4673-4679; (b) S. Deike, W. H. Binder, *Macromolecules* 50 (2017) 2637-2644; (c) Y. Zhang, J. G. Hu, G. Yang, H. L. Zhang, Q. J. Zhang,

- F. Wang, G. Zou, *J. Polym. Sci. Part A* 55 (2017) 2458-2466; (d) M. J. Cho, J. Ahn, Y. Kim, H. A. Um, P. N. Prasad, G. J. Lee, D. H. Choi, *RSC. Adv.* 6 (2016) 23879-23886.
- [3] (a) S. Wang, J. X. Chen, X. Y. Feng, G. Shi, J. Zhang, X. H. Wan, *Macromolecules* 50 (2017) 4610-4615; (b) K. Maeda, S. Wakasone, K. Shimomura, T. Ikai, S. Kanoh, *Macromolecules* 47 (2014) 6540-6546; (c) A. R. A. Palmans, E. W. Meijer, *Angew. Chem. Int. Ed.* 46 (2007) 8948-8968; (d) J. V. Gestel, *Macromolecules* 37 (2004) 3894-3898.
- [4] B. Kunnen, C. Macdonald, A. Doronin, S. Jacques, M. Eccles, I. Meglinski, *J. Biophotonics* 8 (2015) 317-323.
- [5] (a) C. H. Fan, X. M. Huang, L. H. Han, Z. L. Lu, Z. Wang, Y. P. Yi, *Sensor. Actuat. B-Chem.* 224 (2016) 592-599; (b) C. P. Montgomery, B. S. Murray, E. J. New, R. Pal, D. Parker, *Accounts. Chem. Res.* 42 (2009) 925-937.
- [6] T. Kawasaki, M. Sato, S. Ishiguro, T. Saito, Y. Morishita, I. Sato, H. Nishino, Y. Inoue, K. Soai, *J. Am. Chem. Soc.* 127 (2005) 3274-3275.
- [7] J. D. Luo, Z. L. Xie, J. W. Y. Lam, L. Cheng, H. Y. Chen, C. F. Qiu, H. S. Kwok, X. W. Zhan, Y. Q. Liu, D. B. Zhu, B. Z. Tang, *Chem. Commun.* 28 (2001) 1740-1741.
- [8] (a) L. C. Mao, X. H. Liu, M. Y. Liu, L. Huang, D. Z. Xu, R. M. Jiang, Q. Huang, Y. Q. Wen, X. Y. Zhang, Y. Wei, *Appl. Supf. Sci.* 419 (2017) 188-196; (b) M. Y. Liu, H. Y. Huang, K. Wang, D. Z. Xu, Q. Wan, J. W. Tian, Q. Huang, F. J. Deng, X. Y. Zhang, Y. Wei, *Carbohydr. Polym.* 142 (2016) 38-44.
- [9] (a) M. Gao, H. F. Su, S. W. Li, Y. H. Lin, X. Ling, A. J. Qin, B. Z. Tang, *Chem. Commun.* 53 (2017) 921-924; (b) Y. Y. Zhao, R. T. K. Kwok, J. W. Y. Lam, B. Z. Tang, *Nanoscale*, 8 (2016) 12520-12523.

- [10] P. Li, Q. Y. Zeng, H. Z. Sun, M. Akhtar, G. G. Shan, X. G. Hou, F. S. Li, Z. M. Su, *J. Mater. Chem. C* 4 (2016) 10464-10470.
- [11] J. Z. Liu, H. M. Su, L. M. Meng, Y. H. Zhao, C. M. Deng, J. C. Y. Ng, P. Lu, M. Faisal, J. W. Y. Lam, X. H. Huang, H. K. Wu, K. S. Wong, B. Z. Tang, *Chem. Sci.* 3 (2012) 2737-2747.
- [12] J. L. Han, J. You, X. G. Li, P. F. Duan, M. H. Liu, *Adv. Mater.* 29 (2017) 1606503.
- [13] (a) Z. Y. Wang, S. Liu, Y. X. Wang, Y. W. Quan, Y. X. Cheng, *Macromol. Rapid Commun.* 38 (2017) 1700150; (b) Y. X. Wang, Y. Z. Li, S. Liu, C. J. Zhu, S. Li, Y. X. Cheng, *Macromolecules* 49 (2016) 5444-5451; (c) S. W. Zhang, Y. Sheng, G. Wei, Y. W. Quan, Y. X. Cheng, C. J. Zhu, *Polym. Chem.* 6 (2015) 2416-2422.
- [14] (a) R. C. Samanta, H. Yamamoto, *J. Am. Chem. Soc.* 139 (2017) 1460-1463; (b) L. Yang, R. Melot, M. Neuburger, O. Baudoin, *Chem. Sci.* 8 (2017) 1344-1349; (c) Y. D. Zhang, J. P. Wu, G. S. Li, K. R. Fandrick, J. Gao, Z. Tan, J. Johnson, W. J. Li, S. Sanyal, J. Wang, X. F. Sun, J. C. Lorenz, S. Rodriguez, J. T. Reeves, N. Grinberg, H. Lee, N. Yee, B. Z. Lu, C. H. Senanayake, *J. Org. Chem.* 81 (2016) 2665-2669.
- [15] (a) T. Song, Y. Cao, G. Zhao, L. Pu, *Inorg. Chem.* 56 (2017) 4395-4399; (b) J. Y. C. Lim, I. Marques, L. Ferreira, V. Félix, P. D. Beer, *Chem. Commun.* 52 (2016) 5527-5530; (c) Z. Huang, S. Yu, K. Wen, X. Yu, L. Pu, *Chem. Sci.* 5 (2014) 3457-3462.
- [16] (a) W. Y. Wang, X. Y. Ji, Z. M. Du, B. H. Wang, *Chem. Commun.* 53 (2017) 1370-1373; (b) D. Limnios, C. G. Kokotos, *Adv. Synth. Catal.* 359 (2017) 323-328; (c) L. Qu, P. Sun, Y. Wu, K. Zhang, Z. P. Liu, *Macromol. Rapid Comm.* 38 (2017) 1700121; (d) Z. X. Liu, B. B. Chen, M. L. Liu, H. Y. Zou, C. Z. Huang, *Green Chem.* 19 (2017) 1494-1498; (e) W. Liu, S. J. Liu, Y. Q. Kuang, F. Y. Luo, J. H. Jiang, *Anal. Chem.* 88 (2016) 7867-7872; (f) D. Walker, D. P. Singh, P.

Fischer, *Adv. Mater.* 28 (2016) 9846-9850.

[17] (a) H. J. Zheng, T. G. Zhu, X. Q. Li, G. Wang, Q. Jia, *Biomacromolecules* 18 (2017) 3971-3977; (b) J. A. Finbloom, K. Han, C. C. Slack, A. L. Furst, M. B. Francis, *J. Am. Chem. Soc.* 139 (2017) 9691-9697; (c) D. Bini, L. Russo, C. Battocchio, A. Natalello, G. Polzonetti, S. M. Doglia, F. Nicotra, L. Cipolla, *Org. Lett.* 16 (2014) 1298-1301.

[18] (a) N. Liu, C. H. Ma, R. W. Sun, J. Huang, C. L. Li, Z. Q. Wu, *Polym. Chem.* 8 (2017) 2152-2163; (b) G. Yang, Y. Y. Xu, Z. D. Zhang, L. H. Wang, X. H. He, Q. J. Zhang, C. Y. Hong, G. Zou, *Chem. Commun.* 53 (2017) 1735-1738; (c) S. Deike, W. H. Binder, *Macromolecules* 50 (2017) 2637-2644; (d) S. Fukuzawa, H. Oki, M. Hosaka, J. Sugasawa, S. Kikuchi, *Org. Lett.* 9 (2007) 5557-5560.

[19] L. F. Zheng, X. B. Huang, Y. G. Shen, Y. X. Cheng, *Synlett* 3 (2010) 0453-0456.

[20] (a) H. Q. Peng, X. Y. Zheng, T. Han, R. T. K. Kwok, J. W. Y. Lam, X. Huang, B. Z. Tang, *J. Am. Chem. Soc.* 139 (2017) 10150-10156; (b) J. Wang, J. Mei, E. Zhao, Z. G. Song, A. J. Qin, J. Z. Sun, B. Z. Tang, *Macromolecules* 45 (2012) 7692-7703; (c) M. Minato, P. M. Lahti, *J. Am. Chem. Soc.* 119 (1997) 2187-2195.

[21] L. D. Bari, G. Pescitelli, P. Salvadori, *J. Am. Chem. Soc.* 121 (1999) 7998-8004.

[22] (a) H. K. Li, X. Y. Zheng, H. M. Su, J. W. Y. Lam, K. S. Wong, S. Xue, X. J. Huang, X. H. Huang, B. S. Li, B. Z. Tang, *Scientific Reports* 6 (2016) 19277; (b) G. Singh, H. Chan, A. Baskin, E. Gelman, N. Repnin, P. Král, R. Klajn, *Science* 345 (2014) 1149-1153; (c) Z. C. Zuo, H. B. Liu, X. D. Yin, H. Y. Zheng, Y. L. Li, *J. Colloid. Interf. Sci.* 329 (2009) 390-394; (d) L. Zhang, E. Ruh, D. Grützmacher, *Nano Lett.* 6 (2006) 1311-1317.

[23] J. F. Li, C. L. Yang, C. Huang, Y. Wan, W. Y. Lai, *Tetrahedron Lett.* 57 (2016) 1256-1260.

- [24] (a) J. M. Yu, T. Sakamoto, K. Watanabe, S. Furumi, N. Tamaoki, Y. Chen, T. Nakano, Chem. Commun. 47 (2011) 3799-3801; (b) Y. Nakano, Y. Liu, M. Fujiki, Polym. Chem. 1 (2010) 460-469; (c) K. Watanabe, I. Osaka, S. Yorozuya, K. Akagi, Chem. Mater. 24 (2012) 1011-1024.

ACCEPTED MANUSCRIPT

Highlights

- Two chiral conjugated polymer enantiomers **R-P** and **S-P** were designed and synthesized *via* click polymerization.
- The resulting polymers exhibit obvious AIE behavior.
- These two polymers can exhibit CPL emission signals in the aggregates and cast-spin films, and the highest g_{lum} value can be up to 6.97×10^{-3} and 1.45×10^{-2} , respectively.